

## Pneumatic Humanoid Robot with Adsorption Mechanisms on the Sole to Realize a Stepping Motion in Badminton

Yoshida, Ryuji

Department of Mechanical Engineering, Kyushu University

Kiguchi, Kazuo

Department of Mechanical Engineering, Kyushu University

Nishikawa, Satoshi

Department of Mechanical Engineering, Kyushu University

<https://hdl.handle.net/2324/7178574>

---

出版情報 : pp.1-6, 2024-01-01. IEEE

バージョン :

権利関係 : © 2024 IEEE. Personal use of this material is permitted. Permission from IEEE must be obtained for all other uses, in any current or future media, including reprinting/republishing this material for advertising or promotional purposes, creating new collective works, for resale or redistribution to servers or lists, or reuse of any copyrighted component of this work in other works.



# Pneumatic Humanoid Robot with Adsorption Mechanisms on the Sole to Realize a Stepping Motion in Badminton

Ryuji Yoshida, Kazuo Kiguchi, *Senior Member, IEEE*, and Satoshi Nishikawa, *Member, IEEE*

**Abstract**— Using robots as badminton training partners, the robots preferred to be humanoid in shape. However, existing humanoid robots lack the tipping stability required to perform badminton footwork. In this research, to improve the tipping stability of humanoid robots, we proposed to install adsorption mechanisms on the sole. The robot with three degrees of freedom (DOFs) on one leg was developed as a preliminary step for the evaluation of the mechanisms. First, the basic characteristics of the adsorption mechanisms were evaluated. The evaluation showed that the tipping stability of the robot was improved. In addition, three motions were performed with the developed robot: maintaining a standing posture, stepping forward, and stepping backward. These motions were realized by using a combination of feedforward control and proportional-integral-differential (PID) control. In the forward stepping motion, the robot achieved a quick approach speed of 1.56 m/s. Also, the estimation of the zero moment point (ZMP) during the motion showed that the robot could be prevented from tipping by the adsorption mechanisms.

## I. INTRODUCTION

Sports robots as training partners have been developed for various sports, such as badminton [1], volleyball [2], and football [3]. These robots can help players to improve their skills. However, these robots are limited in their movements and are only suitable for certain situations in competitions. To use robots as training partners in realistic match scenarios, it is necessary to develop robots that can perform more versatile movements.

We chose badminton as our research theme due to its reputation for high speed. The technology developed through badminton robots can be applied to other sports that involve high speed as well. The initial velocity of a badminton smash is the fastest in ball sports. Therefore, badminton robots are required to operate at high speed and high acceleration. In addition, badminton players need to observe the opponent's movements and predict the trajectory of the shuttlecock. These skills are expected to be developed with practice. Indeed, Abernethy *et al.* showed that expert badminton players can predict the trajectory more accurately than novices [4]. Practicing with a humanoid robot allows the players to practice observing their opponent's movements. This can improve the ability to observe the opponent's movements and predict the direction of the shuttle's flight. The above considerations suggest that humanoid robots with high-speed and high-acceleration movements are required for practicing realistic match scenarios in badminton.

Many badminton robots have been developed. Mori *et al.* developed a high-speed humanoid robot arm driven by pneumatic [5] and by pneumatic and electric [6]. These robots have many degrees of freedom (DoFs) and realize skillful shots. However, these robots are fixed to the stand and cannot move around. In contrast, badminton robots that move on wheels have been developed [7]–[10]. In addition, Yang *et al.* proposed a badminton robot that moves on a rail [11]. For all these robots, due to the different methods of movement from humans, it is not expected an improvement in the player's ability to observe the opponent's movements when used as a training partner.

Several humanoid sports robot studies exist. Xiong *et al.* developed a humanoid robot that plays table tennis [12]. The developed robots have realized continuous rallies with each other. However, they cannot perform step out motions during the rally. Also, Hattori *et al.* developed a humanoid robot that performs fast tennis swing motion [13]. This robot can predict the trajectory of the ball and hit it back. However, the velocity of the racket is about 4m/s, which is slow compared to humans. The problem of these humanoid robots arises from the difficulty of controlling the balance in bipedal robots. Therefore, to perform badminton footwork with bipedal humanoid robots, their tipping stability must be improved. However, there are limitations in improving tipping stability with previous methods. To prevent robots from tipping, zero moment point (ZMP) must be kept in the support polygon, but quick motion makes it difficult. Also, the size of the support polygon usually depends on the sole size. This study proposes a method to improve the tipping stability of robots by binding the foot to the ground.

There are a few methods of binding the foot to the ground, such as spike [14] and adsorption, but since spike damage the ground, adsorption is more suitable for the robot to be developed. There are also several types of adsorption, such as electrostatic adsorption, magnetic adsorption, and suction adsorption. Since electrostatic adsorption [15] is relatively weak and magnetic adsorption [16] can only be used for a limited variety of materials, vacuum adsorption was chosen for the developed robot. Previously, many bipedal robots using suction adsorption mechanisms have been developed [17], [18]. However, they were designed to move on inclined surfaces and are not expected to perform fast movements on horizontal surfaces.

Against the above background, we propose a humanoid robot with vacuum adsorption mechanisms as a robot to realize

\*Research supported by JSPS Grants-in-Aid for Scientific Research JP21K17830.

Ryuji Yoshida is with the Department of Mechanical Engineering, Kyushu University, Fukuoka, 819-0395 Japan, (e-mail, yoshida.ryuji.175@s.kyushu-u.ac.jp)

Kazuo Kiguchi is with the Department of Mechanical Engineering, Kyushu University, Fukuoka, 819-0395 Japan, (e-mail: kiguchi@ieee.org)

Satoshi Nishikawa is with the Department of Mechanical Engineering, Kyushu University, Fukuoka, 819-0395 Japan, (e-mail: nishikawa@mech.kyushu-u.ac.jp)

badminton footwork. By evaluating the actual operation of the developed robot, we demonstrate the effectiveness of the adsorption mechanisms.

## II. PNEUMATIC HUMANOID ROBOT WITH AN ADSORPTION MECHANISM ON THE SOLE

### A. Humanoid robot with adsorption mechanisms

To demonstrate the effectiveness of the adsorption mechanisms, the humanoid leg robot (Fig. 1) was developed by modifying the robot developed by Tanaka *et al.* [19]. The robot has three DoFs on one leg (Fig. 2) and performs human motion in the sagittal plane. The height of the robot is approximately 1.2 m and its weight is approximately 9 kg. The dimensions of the robot and the range of motion of each joint are shown in Fig.3. The robot is driven by eight pressure regulating valves (tecno basic, HOERBIGER), and four tanks (550 mL) are used to store compressed air supplied by an air compressor (6-4, JUN-AIR). These components serve as a buffer to prevent pressure drops and ensure the stable operation of the robot. The angle of each joint is measured by potentiometers (3382G-1-103G, Bourns).

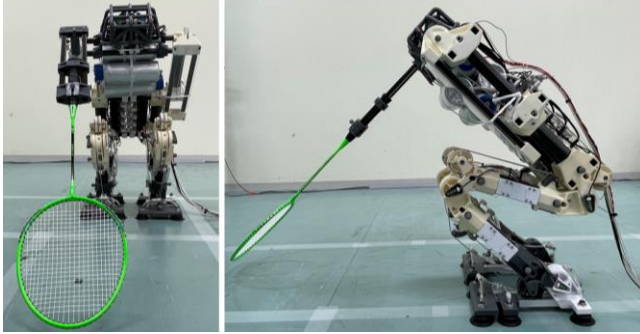


Figure 1. Overview of the developed robot

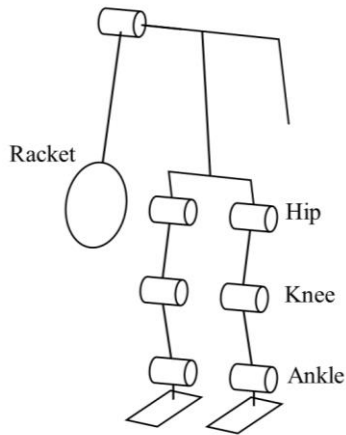


Figure 2. DoF diagram of the developed robot

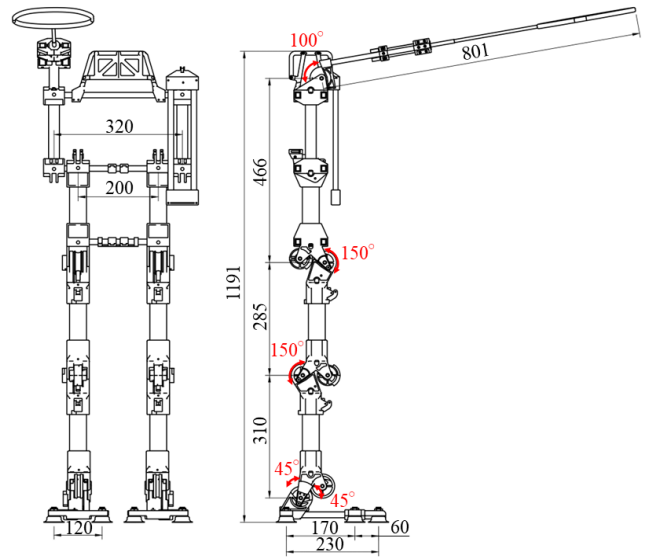


Figure 3. Dimension and range of motion of the robot

### B. Actuator

To achieve high speed and high acceleration movements, such as footwork in badminton, the robot needs to be lightweight. Therefore, Structure Integrated Pneumatic Cable (SIPC) cylinder (Fig.4) was chosen as the actuator of the robot. The actuator is characterized by a high power-to-weight ratio. In addition, since the actuators are part of the structure, the weight of the robot can be light.

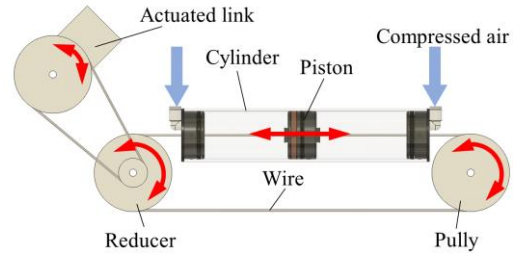


Figure 4. SIPC cylinder

However, power transmission by wire has disadvantages such as limited operating range and slow response. In addition, air compression and expansion cause time delays. Therefore, slow response can particularly be a serious problem. The delay in response time during the wire drive is caused by the looseness of the wire. Therefore, to keep the wire tight, wire tensioners are attached to the wire. The wire tensioners developed are shown in Fig.5.

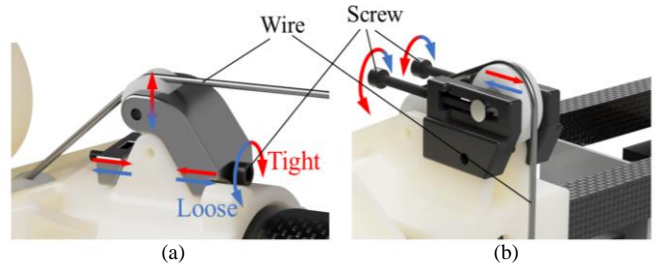


Figure 5. Wire tensioners (a) at the ankle and the knee and (b) at the hip

### C. Adsorption Mechanism

Five suction cups (VPA50RN-6J, PISCO) are attached to each foot of the robot on the left and right sides (Fig.6 (a)). When the robot stands on one leg, the center of mass is located medially in the foot. To enhance stability under such conditions, three suction cups are installed on the lateral side of the foot. A vacuum valve (V112E1, KOGANEI) is installed on each leg, which allows the left and right foot to switch between adsorption and desorption separately. Each vacuum valve is connected to a single vacuum pump (LS-90H, MALUS). The vacuum pump is placed outside of the robot and supplies vacuum to the robot through a tube. Also, to keep the direction of air flow, check valves (AKH06-00, SMC) are installed on each leg. Fig.6 (b) shows the diagram of the vacuum circuit.

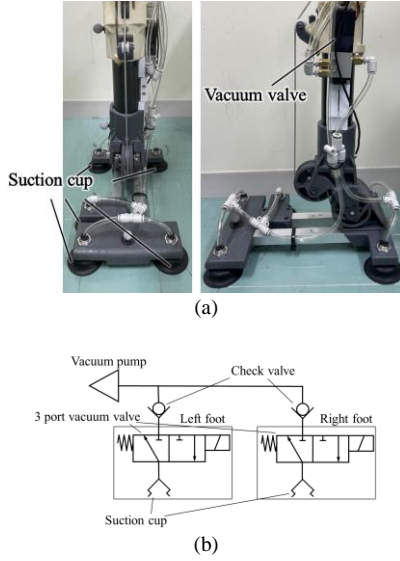


Figure 6. (a) Design of right foot component and (b) vacuum circuit diagram

## III. CHARACTERIZATION OF ADSORPTION MECHANISMS

### A. Pressure Changes during Adsorption and desorption

To control the robot, it is necessary to investigate the forces of the adsorption mechanism and the time required for adsorption and desorption. The following characteristics were investigated by measuring the pressure near the suction cups of the right foot. A pressure sensor (MPS-V34R-NGA, CONVUM) was used to measure the pressure. The pressure was measured by connecting to suction cups of the right foot (Fig.7).



Figure 7. Pressure measurement experiment setting

Due to the use of a single vacuum pump for the adsorption mechanism on each foot, the characteristics of the adsorption

mechanism may vary depending on the contact between the foot and the ground. Therefore, the pressure was measured under the following four conditions.

- [A]. With both feet on the ground, only the right foot is adsorbed or desorbed.
- [B]. With only the right foot on the ground, only the right foot is adsorbed or desorbed.
- [C]. With both feet on the ground, both feet are adsorbed or desorbed.
- [D]. With only the right foot on the ground, both feet are adsorbed or desorbed.

Only the right foot on the ground means that the suction cups of the left foot were separated from the ground by about 5mm, and the right foot remained on the ground. In each condition, the desorption command was given after a sufficient time had elapsed from the start of adsorption.

The pressure changes during adsorption and desorption are shown in Fig.8. In each graph, the command to start adsorption or desorption is set to 0 ms. Fig.8 (a) shows the pressure change during adsorption. There is little difference between the pressure changes for conditions [A] and [B]. This indicates that the vacuum valve sufficiently shuts off the air when it is closed. Comparing conditions [A] and [C], [C] takes more time to reduce the pressure. This is due to the differences in the amount of air being exhausted. In condition [A], the air is exhausted from five suction cups, while in condition [C], the air is exhausted from ten suction cups. Since the amount of air that the vacuum pump can exhaust per unit time is limited, the more suction cups that are vacuumed at the same time, the longer time is required to reduce pressure. In condition [D], since vacuum leakage occurs at the left foot suction cups, the pressure is not reduced as much as in the other conditions. Therefore, the opening timing of the valve on the side of the suction cups off the ground is important. Fig.8 (b) shows the pressure change during desorption. There is little difference among conditions [A], [B], and [C]. Since each of the left and right vacuum valves is released to the atmosphere during desorption, the time required for desorption does not depend on the state of adsorption of the opposite foot.

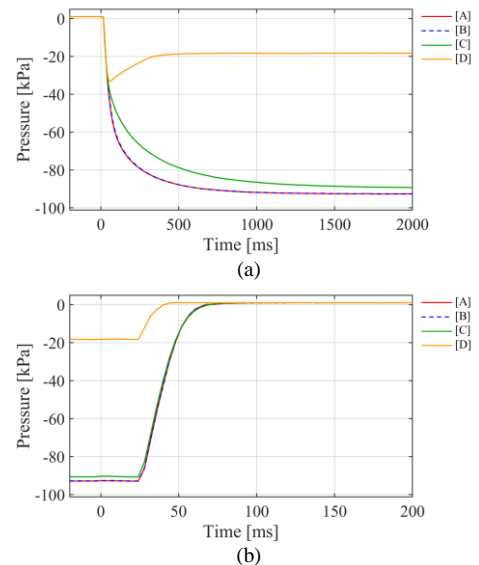


Figure 8. Pressure changes during adsorption (a) and desorption (b)

### B. Estimating the Posture that can be Maintained by the Adsorption Mechanisms

A static posture that the robot can maintain on one leg is estimated based on the measured pressure Fig.8 (a). The robot is modeled as a one DoF mass system for analysis (Fig.8). The mass of the modeled robot is  $m$  [kg], the distance between the mass point and the ankle joint is  $h$  [m], the angle from the vertical direction is  $\theta$  [rad], and the distance from the toe to each suction cup is  $l_1$  [m],  $l_2$  [m],  $l_3$  [m].

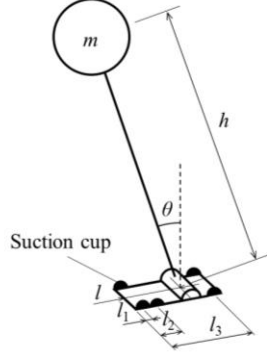


Figure 9. Robot model

Defining the pressure inside the suction cup as  $-P$  [Pa] and the radius of the suction cup as  $r$  [m], the adsorption force  $F$  [N] per suction cup and the moment  $M$  [Nm] generated by the adsorption mechanism of the foot at the toe are expressed as follows.

$$F = P \pi r^2 \quad (1)$$

$$M = F (2 l_1 + l_2 + 2 l_3) \quad (2)$$

The condition that the modeled robot does not fall over when it is static is

$$S m g (h \sin \theta - l) < M, \quad (3)$$

where  $S$  is a safety factor,  $g$  [m/s<sup>2</sup>] is the gravitational acceleration, and  $l$  [m] is the length from the toe to the ankle.

For the developed robot,  $r = 0.025$  [m],  $l_1 = 0.020$  [m],  $l_2 = 0.080$  [m],  $l_3 = 0.25$  [m],  $l = 0.21$  [m],  $h = 0.7$  [m],  $m = 8.2$  [kg]. Substituting these into (1), (2), and (3), the relationship between time and the posture that the robot can maintain is determined. Substituting  $S = 1.5$  to calculate the relationship between the time and the maximum angle that the robot can maintain statically obtained from (3) (Fig.10).

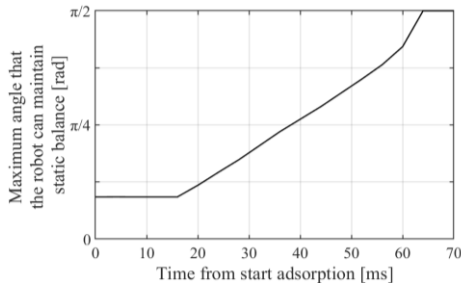


Figure 10. The posture that the robot can maintain

On the right side of the graph in Fig.10, the robot can maintain a static leaning forward posture with only the adsorption of one leg. Therefore, at the pressure reached after

about 70ms from the start of adsorption, the robot can maintain any static posture. Fig.11 shows the robot maintaining a lean forward posture with only the left foot adsorbed.

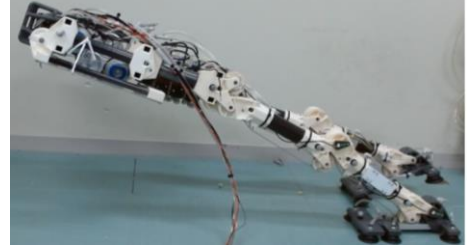


Figure 11. Maintaining a lean forward posture

## IV. EVALUATION EXPERIMENT

Evaluate the performance of the robot through the actual motion. The robot performed initial posture maintenance, forward stepping, and backward stepping. A motion capture system (OptiTrack, Natural Point) was used to measure the motion. Eight motion-capture cameras (Prime13W, Natural Point) were installed to measure the markers attached to the robot. In addition, an RGB camera (C920n, Logitech) was used to record the motion of the robot. The experimental setting is shown in Fig.12. The origin is defined as the left ankle of the robot.

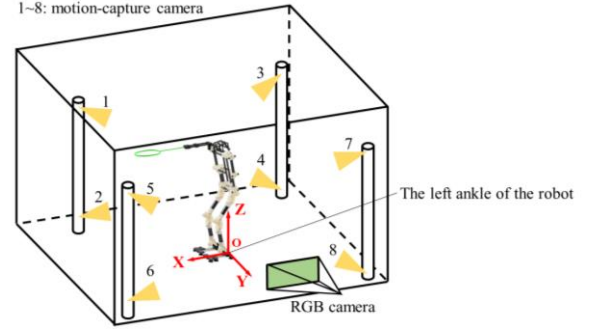


Figure 12. Evaluation experiment setting

### A. Reproducibility of initial posture

To perform the stepping motion in badminton, first, maintain a standing posture as the initial position. Using proportional-integral-differential (PID) control to control the joint angles of the robot. Human support was provided as necessary to ensure a smooth transition from the sitting to the standing posture since the robot exhibited instability while in the sitting posture. Fig.13 shows the initial posture of the motion.

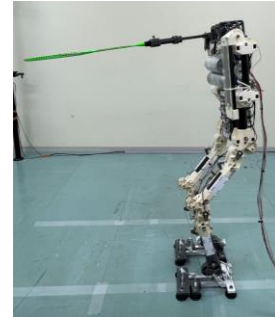


Figure 13. The initial posture of the motion



Evaluate the reproducibility of the motion using the coordinates of the right shoulder of the robot. Fig.14 shows the coordinates just before the stepping motion while maintaining the standing posture four times.

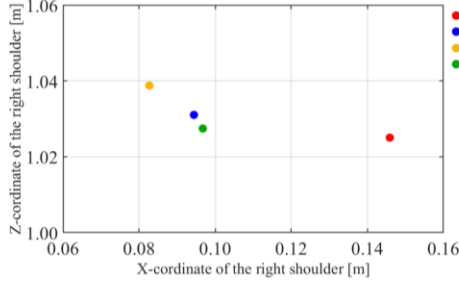


Figure 14. Coordinates of the right shoulder

The difference in shoulder coordinates was about 60 mm at the point of largest difference. As an initial posture for stepping out, it is considered to have sufficient reproducibility. Also, an ideal robot is required to be in the same state in the same posture. Therefore, the reproducibility of the differential pressure at which the robot maintains the initial posture is expected. However, no reproducibility was found for the pressure inside the actuators. At the points where the differential pressures vary the most, the variance is about 130 kPa. The reason for this is that the PID control determines the input based on the position and does not take the pressure into account. SIPC cylinders have high friction and may have different pressure even in the same posture.

### B. Forward Stepping Motion

Due to the slow response and high friction of SIPC cylinders, it is difficult to perform complex motions using PID control. Therefore, feedforward control and PID control are combined to perform a stepping motion. Each joint is controlled by switching between the two control methods at predetermined timings. Fig.15 shows the forward stepping motion.

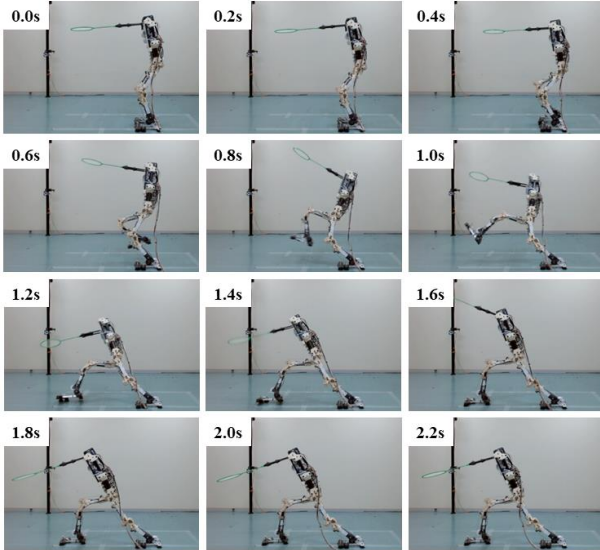


Figure 15. Forward stepping motion

Estimate the ZMP during the stepping motion by modeling the robot as a single mass system. When the robot moves in

the XZ plane, the X coordinate of the ZMP, denoted as  $x_{ZMP}$  [m], is given by

$$x_{ZMP} = x + \frac{z \ddot{x}}{\ddot{z} + g}, \quad (4)$$

where  $x$  [m] is the X coordinate of the mass point,  $z$  [m] is the Z coordinate of the mass point, and  $g$  [m/s<sup>2</sup>] is the gravitational acceleration. The relationship between time and the ZMP during the forward stepping is shown in Fig.16. The areas of the red and blue lines indicate the support polygon and  $y_{ZMP}$  is the Y-coordinate of the ZMP. The ZMP in the X-axis direction and the Y-axis direction is out of the support polygon. Although the ZMP is out of the support polygon, the robot performed the forward stepping without tipping. This indicates that the adsorption mechanism prevented the robot from tipping.

The forward stepping motion was performed three times. The width of the stride was approximately 0.70 – 0.77 m, and the approach speed was approximately 0.98 – 1.56 m/s. The approach speed is defined as the average speed from the starting position to the initial contact of the foot with the ground. Comparison with human motion in terms of the width or the stride and approach speed. The width of the stride of male badminton players is 0.83 – 0.87 m [20], and the approach speed of badminton players is 1.5 – 2.5 m/s [21]. Considering the difference in height between the robot and the human, the width of the stride is large enough compared to that of the human. On the other hand, its approach speed is inferior to that of the human. However, since the command values are determined by trial and error and not the best value, the approach speed can be improved by using better control methods. Also, the robot can perform larger stride stepping motion by other command value.

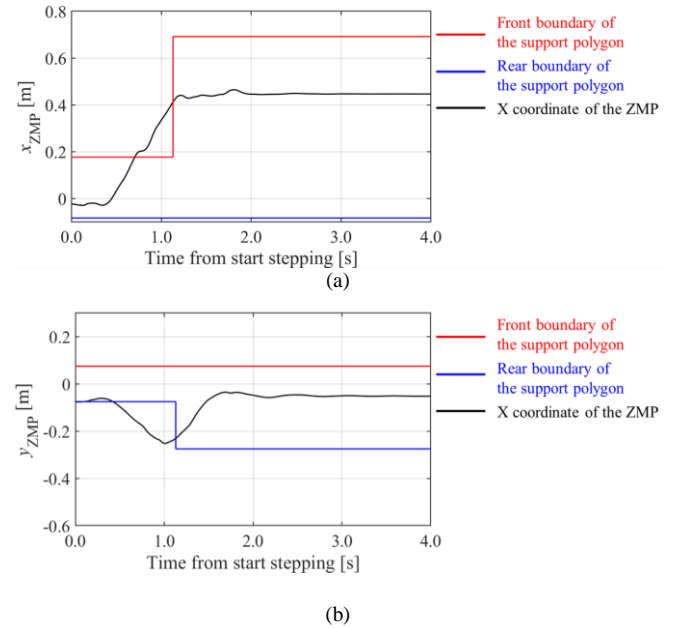


Figure 16.  $x_{ZMP}$  (a) and  $y_{ZMP}$  (b) during the forward stepping

### C. Backward stepping motion

As with the forward stepping, a combination of feedforward control and PID control was used for the

backward stepping. Fig.17 shows the backward stepping motion.

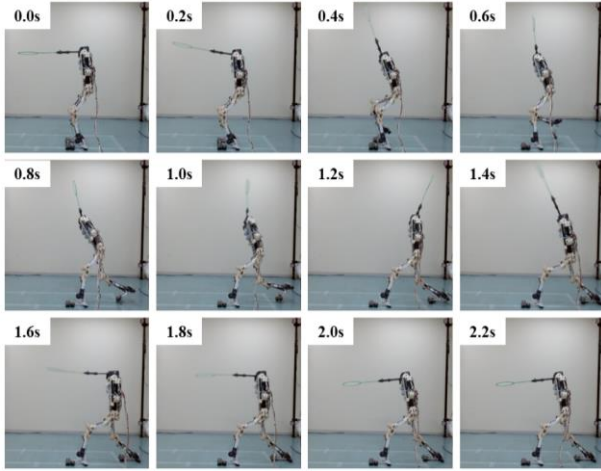


Figure 17. Backward stepping motion

During the backward stepping, the ZMP in the X-axis direction was in the support polygon. However, the ZMP in the Y-axis direction was out of the support polygon (Fig.18). The adsorption mechanism contributed to preventing the robot from tipping. Three times the motion was performed, the width of the stride was approximately 0.46 – 0.69 m.

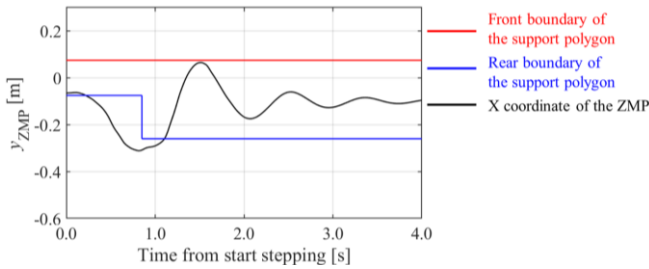


Figure 18.  $y_{ZMP}$  during the backward stepping

## V. CONCLUSION

We developed a humanoid robot with adsorption mechanisms to demonstrate the effectiveness of improving tipping stability. The characteristics of the adsorption mechanism were investigated, and it was confirmed that the tipping stability of the robot was improved. The motion of the robot was also evaluated. The robot was able to maintain the standing posture by PID control. Estimation of the ZMP assuming no adsorption mechanism confirmed that the ZMP was out of the support polygon during forward stepping and backward stepping. Nonetheless, the robot successfully performed stepping motions without tipping, suggesting that the adsorption mechanism prevented tipping. The robot achieved a maximum approach speed of 1.56 m/s during forward stepping, but it was inferior to that of badminton players.

In the future, by improving the control method, higher reproducibility of motion and stepping speed comparable to that of humans will be realized. In addition, since the robot can only move in the sagittal plane, increasing the DoFs of the legs will enable the robot to move in all directions and to jump.

## REFERENCES

- [1] T. T. Tung, N. X. Quynh, and T. V. Minh, "A prototype of auto badminton training robot," *Results in Engineering*, vol. 13, p. 100344, 2022.
- [2] K. Sato, K. Watanabe, S. Mizuno, M. Manabe, H. Yano, and H. Iwata, "Development and assessment of a block machine for volleyball attack training," *Advanced Robotics*, vol. 31, no. 21, pp. 1144–1156, Nov. 2017.
- [3] "MVP Dummy | Robotic Sports Training Equipment." <https://www.mvpdummy.com/> (accessed Nov. 08, 2022).
- [4] B. Abernethy and D. G. Russell, "The relationship between expertise and visual search strategy in a racquet sport," *Hum Mov Sci*, vol. 6, no. 4, pp. 283–319, 1987.
- [5] S. Mori, K. Tanaka, S. Nishikawa, R. Niiyama, and Y. Kuniyoshi, "High-Speed and Lightweight Humanoid Robot Arm for a Skillful Badminton Robot," *IEEE Robot Autom Lett*, vol. 3, no. 3, pp. 1727–1734, Jul. 2017.
- [6] S. Mori, K. Tanaka, S. Nishikawa, R. Niiyama, and Y. Kuniyoshi, "High-Speed Humanoid Robot Arm for Badminton Using Pneumatic-Electric Hybrid Actuators," *IEEE Robot Autom Lett*, vol. 4, no. 4, pp. 3601–3608, 2019.
- [7] W. Sun, J. Kong, X. Wang, and H. Liu, "Badminton robot batting mechanism design and badminton trajectory simulation," *IOP Conf Ser Mater Sci Eng*, vol. 493, no. 1, p. 012019, 2019.
- [8] N. Mizuno *et al.*, "Development of Automatic Badminton Playing Robot with Distance Image Sensor," *IFAC-PapersOnLine*, vol. 52, no. 8, pp. 67–72, 2019.
- [9] W. Chen *et al.*, "Using FTOC to track shuttlecock for the badminton robot," *Neurocomputing*, vol. 334, pp. 182–196, Mar. 2019.
- [10] J. Yang, X. Ji, and L. Ying, "Stochastic energy saving strategies using machine learning for badminton robots," *Aggression and Violent Behavior*. Elsevier Ltd, 2021.
- [11] J. Stoev, S. Gillijns, A. Bartic, and W. Symens, "Badminton playing robot - a multidisciplinary test case in Mechatronics," *IFAC Proceedings Volumes*, vol. 43, no. 18, pp. 725–731, 2010.
- [12] R. Xiong, Y. Sun, Q. Zhu, J. Wu, and J. Chu, "Impedance control and its effects on a humanoid robot playing table tennis," *Int J Adv Robot Syst*, vol. 9, Nov. 2012.
- [13] M. Hattori *et al.*, "Fast Tennis Swing Motion by Ball Trajectory Prediction and Joint Trajectory Modification in Standalone Humanoid Robot Real-time System," in *2020 IEEE/RSJ International Conference on Intelligent Robots and Systems (IROS)*, 2020, pp. 3612–3619.
- [14] J. S. Lee, M. Plecnik, J.-H. Yang, and R. S. Fearing, "Self-Engaging Spined Gripper with Dynamic Penetration and Release for Steep Jumps," 2018 IEEE International Conference on Robotics and Automation (ICRA), 2018.
- [15] R. Chen, "A Gecko-Inspired Electrodeposited Wall-Climbing Robot," *Potentials, IEEE*, vol. 34, pp. 15–19, Apr. 2015.
- [16] J. Fan, T. Xu, Q. Fang, J. Zhao, and Y. Zhu, "A Novel Style Design of a Permanent-Magnetic Adsorption Mechanism for a Wall-Climbing Robot," *J Mech Robot*, vol. 12, no. 3, Feb. 2020.
- [17] H. Zhu, Y. Guan, W. Wu, L. Zhang, X. Zhou, and H. Zhang, "Autonomous pose detection and alignment of suction modules of a biped wall-climbing robot," *IEEE/ASME Transactions on Mechatronics*, vol. 20, no. 2, pp. 653–662, Apr. 2015.
- [18] X. Shi *et al.*, "A 6-DOF humanoid wall-climbing robot with flexible adsorption feet based on negative pressure suction," *Mechatronics*, vol. 87, p. 102889, 2022.
- [19] K. Tanaka, S. Nishikawa, R. Niiyama, and Y. Kuniyoshi, "Immediate Generation of Jump-and-Hit Motions by a Pneumatic Humanoid Robot Using a Lookup Table of Learned Dynamics," *IEEE Robot Autom Lett*, vol. 6, no. 3, pp. 5557–5564, Jul. 2021.
- [20] A. M. Nadzalan, S. H. Azmi, N. I. Mohamad, J. L. F. Lee, K. Tan, and C. Chinnasee, "Kinematics analysis of dominant and non-dominant lower limb during step and jump forward lunge in badminton," *Journal of Fundamental and Applied Sciences*, vol. 10, no. 3S, pp. 232–242, 2018.
- [21] R. Valdecabres, A. de Benito Trigueros, G. Littler, and J. Richards, "An exploration of the effect of proprioceptive knee bracing on biomechanics during a badminton lunge to the net, and the implications to injury mechanisms," *PeerJ*, vol. 6, Dec. 2018.